

Technical Note

Predicting Uniaxial Compressive Strength by Point Load Test: Significance of Cone Penetration

By

A. Basu and A. Aydin

Department of Earth Sciences, The University of Hong Kong,
Hong Kong SAR, China

Received July 15, 2005; accepted January 3, 2006
Published online March 30, 2006 © Springer-Verlag 2006

Keywords: Point load test, cone penetration, uniaxial compressive strength, weathering grade, granite.

1. Introduction

Uniaxial compressive strength (UCS) is considered as one of the key properties in characterization of rock materials in engineering practice. As the standard laboratory tests to determine UCS require machined specimens, indirect tests are often used to predict UCS. “The possibility of using relatively unprepared specimens for a rock strength test has always been attractive, and for this the point load test seems potentially the most useful” (Brook, 1985). The test involves loading core specimens or irregular rock fragments between the conical platens and measuring the applied force (P_f) and the distance (D_f) between the platens *at failure*. These measurements provide an index of tensile strength that can be empirically related to UCS. This study explores why and how accurate measurement of D_f improves the reliability of point load strength index in predicting UCS.

In practice, however, the commercial point load test systems are not equipped to measure D_f , which is consequently assumed to be the initial distance (D_i) by ignoring possible cone penetration and reduction in D_i . The influence of cone penetration on the reliability of point load test in predicting UCS was mentioned in the literature but was not experimentally investigated. This study explored the changes and magnitudes of cone penetration with weathering in granitic specimens, and the significance of these changes on the performance of point load test to consistently produce a smaller band of scatter, and hence improve prediction of UCS and the weathering grade.

2. Background

In point load testing, rock specimens (cylindrical, prismatic or irregular) loaded between two conical platens (of stipulated geometry and hardness) fail by development of one or more extensional planes containing the line of loading. Although the point load test has been studied extensively, the actual stress distribution between the platens is not well-understood (Chau and Wong, 1996). Wijk (1978) obtained the following analytical approximations for the tensile stress at the centre of a diametrically loaded sphere and an axially loaded cylinder, respectively:

$$\sigma_t = -\beta_{\text{sphere}} \frac{P}{D^2}, \quad (1)$$

$$\sigma_t = -\left(\beta_{\text{plate}} + \frac{2D^2\nu}{\pi W^2}\right) \frac{P}{D^2}, \quad (2)$$

where the parameter $\beta_{\text{sphere}} = 0.77-0.89$ and $\beta_{\text{plate}} = 0.39-0.61$ for Poisson's ratio (ν) values of 0.10 and 0.33, P applied load, D distance between loading points, and W diameter of the cylinder.

A similar expression was previously developed by Reichmuth (1968) for the point load tensile strength T_0 :

$$T_0 = K_s \frac{P_f}{D^2} + K_b P_f, \quad (3)$$

where P_f is failure load, and K_s and K_b are empirical shape and brittleness factors respectively. No size effect was evident with this analysis. Broch and Franklin (1972) reviewing the development of the test concluded that Reichmuth's formula Eq. (3) is complex with little practical value and could be simplified to:

$$I_s = \frac{P_f}{D^2} \text{ (MPa)}, \quad (4)$$

where I_s is the point load strength index.

Considerable variations of I_s with specimen size and shape lead Broch and Franklin (1972) to introduce a reference index $I_s(50)$ which corresponds to the I_s of a diametrically loaded rock core of 50 mm diameter. Accordingly, initial I_s values are reduced to $I_s(50)$ by size correction factors determined from empirical curves as a function of D . They indicated that the considerably larger shape effect should be avoided by testing specimens with specified geometries. ISRM (1985) proposed a new correction function which accounts for both size and shape effects by utilizing the concept of 'equivalent core diameter' (D_e). This function (known as geometric correction factor) is given by:

$$F = (D_e/50)^{0.45}. \quad (5)$$

Suggested methods by ISRM (1985) and ASTM (2001) for determining $I_s(50)$ comply completely where the index is given by:

$$I_s(50) = F \times \frac{P_f}{D_e^2} \text{ (MPa)}. \quad (6)$$

It is clear that the induced tensile stress under point loading is a function of D . Broch and Franklin (1972) indicated that D at the instant of failure equals to that at the start of the test only if the specimen is hard and platens do not penetrate into the

specimen. ISRM (1985) and ASTM (2001) also specify that the error by taking D to be the initial distance measured prior to loading is negligible when the specimen is large or strong. On the contrary, our observations during the earlier point load tests showed that cone penetration depth in fresh/strong rocks may not be negligible as suggested in the standards. Therefore, this study was designed to investigate significance of measuring cone penetration depth. A laser sensor was used to detect the distance between the conical platens at the instant of failure, which led to a significant improvement in predicting UCS.

3. Experiments, Data Analysis and Discussion

The investigation included testing of a total of 40 granitic (compositionally monzogranite) air-dried core specimens of various weathering grades (ranging from Grade I to IV as confirmed by both macro- and microscopic examinations) (Table 1). Length-diameter

Table 1. Weathering grades and descriptions of investigated granitic rocks (average grain size 3.30–4.20 mm)

Grade	Characteristics of rock core	Microfabric features
I (Parent rock)	<ul style="list-style-type: none"> • No discoloration • Grains have vitreous luster • Equigranular texture with intact grain boundaries 	<ul style="list-style-type: none"> • Equigranular phaneritic texture and intact grain boundaries • Partial sericitization (duteric alteration) of plagioclase • Fresh quartz, K-feldspar and biotite • Occasional intra-granular microcracks in quartz
I–II	<ul style="list-style-type: none"> • Minor discoloration • Grains have vitreous to sub-vitreous luster • Intact grain boundaries 	<ul style="list-style-type: none"> • Minor staining • Slight sericitization and chloritization of plagioclase and biotite respectively • Fresh quartz and K-feldspar • More intragranular microcracks in quartz • Some transgranular microcracks
II	<ul style="list-style-type: none"> • Slight discoloration • Grains have sub-vitreous to dull luster • Intact grain boundaries • Not easily broken by a geological hammer 	<ul style="list-style-type: none"> • Slight staining • Moderate sericitization of plagioclase • Slight to moderate chloritization of biotite • Fresh quartz and K-feldspar • Abundant intragranular microcracks in quartz • Frequent transgranular microcracks
III	<ul style="list-style-type: none"> • Moderately discolored • Soft white clay minerals can be scratched by nail • Grain boundaries not very intact • Can be broken by one firm blow of a geological hammer 	<ul style="list-style-type: none"> • High degree of staining • High to complete sericitization of plagioclase • Phylloporo-meso-alteromorph after biotite • Slight to moderate decomposition of K-feldspar • Disintegrated quartz in places
III–IV	<ul style="list-style-type: none"> • Moderately to highly decomposed and discolored (more gritty and clayey appearance of feldspars) • Can be broken by one light blow of a geological hammer 	<ul style="list-style-type: none"> • Very high degree of staining • Relict plagioclase and biotite • Moderately decomposed K-feldspar • Highly disintegrated quartz
IV	<ul style="list-style-type: none"> • Highly decomposed and discolored with loose grain boundaries • NX core can be broken by hand • Does not readily slake in water 	<ul style="list-style-type: none"> • Moderately to highly decomposed K-feldspar • Extremely disintegrated appearance of quartz

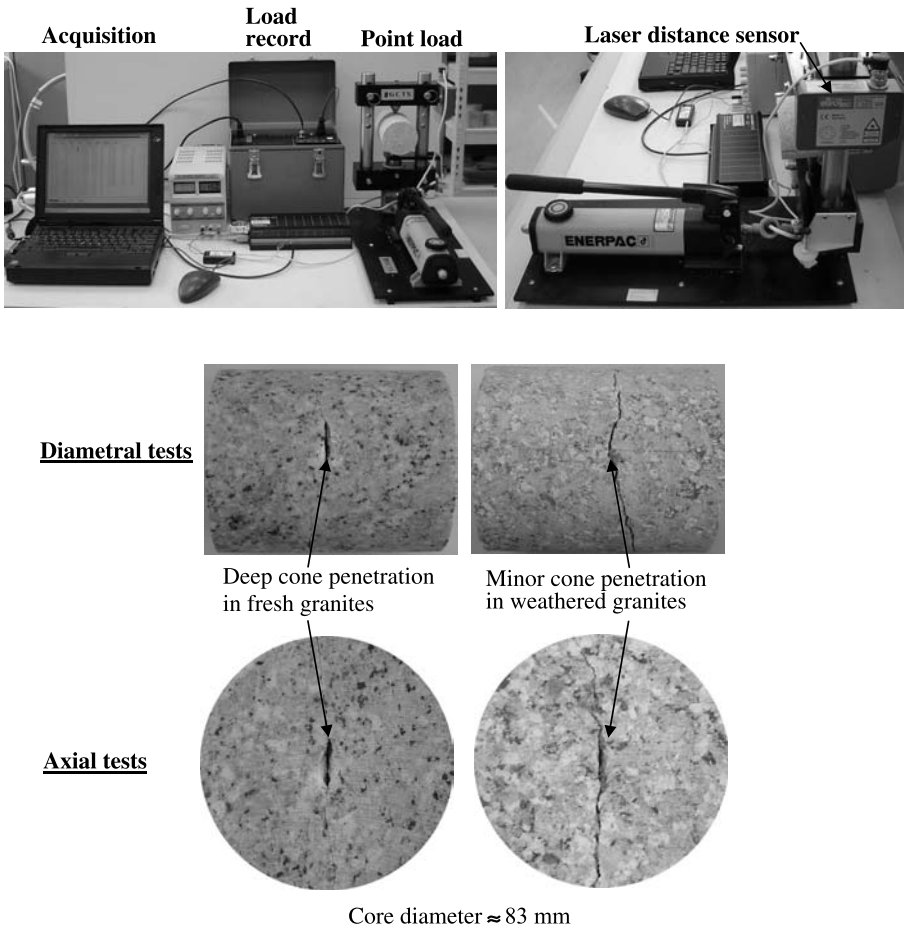


Fig. 1. Laboratory setup for the point load test and failed specimens

ratios of the specimens were within the ISRM (1985) and ASTM (2001) specifications. The specimens were loaded either axially or diametrically and only those failed in one of the valid modes were considered in the analysis (Fig. 1). A laser distance sensor (sampling period: 0.19 sec.; accuracy = 0.05 mm) was attached to the GCTS[®] point load test frame to measure the distance between the conical platens from the beginning of the test to the moment of failure (Fig. 1). A data acquisition system was used to continuously record the load (P) and the platen distance (D) (Fig. 1). Point load strength index $I_s(50)$ of each specimen was calculated from Eq. (6) using both initial (D_i) and final (D_f) platen distances (Table 2).

Uniaxial compressive strengths (UCS) of equivalent air-dried specimens (length-diameter ratio $\approx 2:1$) were determined to be correlated with $I_s(50)_i$ and $I_s(50)_f$ (Table 2). It was found that both relationships were linear but the correlation was significantly better for $I_s(50)_f$ (Fig. 2a). As mentioned before, the standards (ISRM and ASTM) stipulate that if significant cone penetration occurs during the test, such as

Table 2. Weathering grade, grain size, $I_s(50)$ and UCS

SN	WG	d_g (mm)	Load	W (mm)	D_i (mm)	D_f (mm)	P_f (kN)	$I_s(50)_i$ (MPa)	$I_s(50)_f$ (MPa)	σ_{UCS} (MPa)
1	I	3.56	a	83.70	70.21	51.14	39.84	6.81	8.71	196.45
2	I	3.48	a	83.35	62.10	52.32	37.96	7.16	8.18	160.20
3	I	3.73	d	–	84.87	69.09	37.85	6.67	7.82	157.22
4	I	4.14	a	83.50	57.79	43.15	31.56	6.29	7.88	155.70
5	I	3.30	a	83.65	81.65	71.97	49.49	7.53	8.31	148.36
6	I	3.43	a	83.80	73.20	66.96	45.94	7.60	8.14	136.15
7	I	3.30	a	83.70	67.82	62.31	44.68	7.85	8.38	133.55
8	I	3.68	a	83.00	62.99	54.70	35.09	6.57	7.33	123.25
9	I	3.72	a	83.75	28.72	19.23	15.26	5.21	7.12	139.45
10	I	3.67	a	84.00	65.00	56.86	37.69	6.82	7.57	121.40
11	I	3.70	a	83.55	65.94	59.71	32.98	5.93	6.40	116.30
12	I–II	3.73	a	84.00	64.67	56.91	32.66	5.94	6.55	106.34
13	I–II	3.40	a	60.25	58.23	50.76	16.40	4.18	4.65	88.20
14	I–II	3.79	a	83.50	66.36	54.33	18.56	3.32	3.88	83.13
15	II	3.87	d	–	60.31	55.45	12.87	3.85	4.11	68.21
16	II	4.08	a	83.30	29.40	26.40	8.80	2.97	3.22	59.36
17	II	4.08	a	83.45	82.55	72.68	17.00	2.57	2.84	53.19
18	II	4.08	d	–	60.38	55.49	8.02	2.40	2.56	45.67
19	II	3.98	d	–	60.46	57.06	5.51	1.64	1.72	32.16
20	II	3.95	d	–	60.32	56.64	6.86	2.05	2.15	31.14
21	III	4.12	a	83.70	33.80	32.86	6.06	1.83	1.87	26.83
22	III	4.14	d	–	83.57	81.31	7.74	1.40	1.43	24.35
23	III	4.13	d	–	83.68	78.67	7.01	1.26	1.32	22.96
24	III	3.99	d	–	83.75	80.05	6.52	1.17	1.21	22.32
25	III	3.81	d	–	82.96	81.01	5.04	0.92	0.94	14.70
26	III	3.88	d	–	83.44	77.63	4.36	0.79	0.83	13.66
27	III	3.98	d	–	83.76	80.41	4.56	0.82	0.85	13.61
28	III–IV	3.60	d	–	83.06	74.36	5.00	0.91	0.99	18.84
29	III–IV	4.02	d	–	83.66	82.15	3.52	0.63	0.64	17.30
30	III–IV	3.91	d	–	83.48	78.89	2.73	0.49	0.52	7.64
31	III–IV	3.98	d	–	83.55	78.06	6.84	1.17	1.30	23.15
32	III–IV	3.66	a	83.65	77.16	73.46	4.93	0.78	0.81	19.70
33	III–IV	3.96	a	83.65	33.80	29.86	4.54	1.37	1.51	25.14
34	III–IV	4.17	a	83.60	59.72	55.56	3.62	0.70	0.74	22.16
35	III–IV	3.77	d	–	83.75	78.40	3.87	0.70	0.73	11.67
36	IV	4.20	a	83.50	68.30	67.07	1.98	0.35	0.35	6.32
37	III–IV	2.41	a	83.00	54.14	42.04	7.29	1.54	1.87	33.86
38	III–IV	2.45	d	–	83.00	68.38	11.66	2.12	2.46	41.73
39	IV	2.32	a	83.55	83.37	78.95	7.73	1.16	1.21	25.38
40	IV	2.37	d	–	83.82	80.79	4.92	0.88	0.91	22.66

Abbreviations: SN = specimen; WG = weathering grade; d_g = average grain size; a = axial; d = diametral; W = specimen width; D = distance between platens; i = initial; f = final; P_f = failure load; $I_s(50)$ = point load strength index; σ_{UCS} = uniaxial compressive strength.

when testing weak sandstones, the value of D should be the final value of the separation of the loading points. However, this study showed that cone penetration is much deeper in fresher/stronger granites compared to the weathered ones (Fig. 1), and should not be ignored where its measurement is possible. In accordance with this observation, it was also noted that in most of the published correlations between $I_s(50)_i$ and UCS, the scatter in the data increases with UCS, which is more pronounced in those correlations involving a variety of rock types (Figs. 2b–f). It is believed that

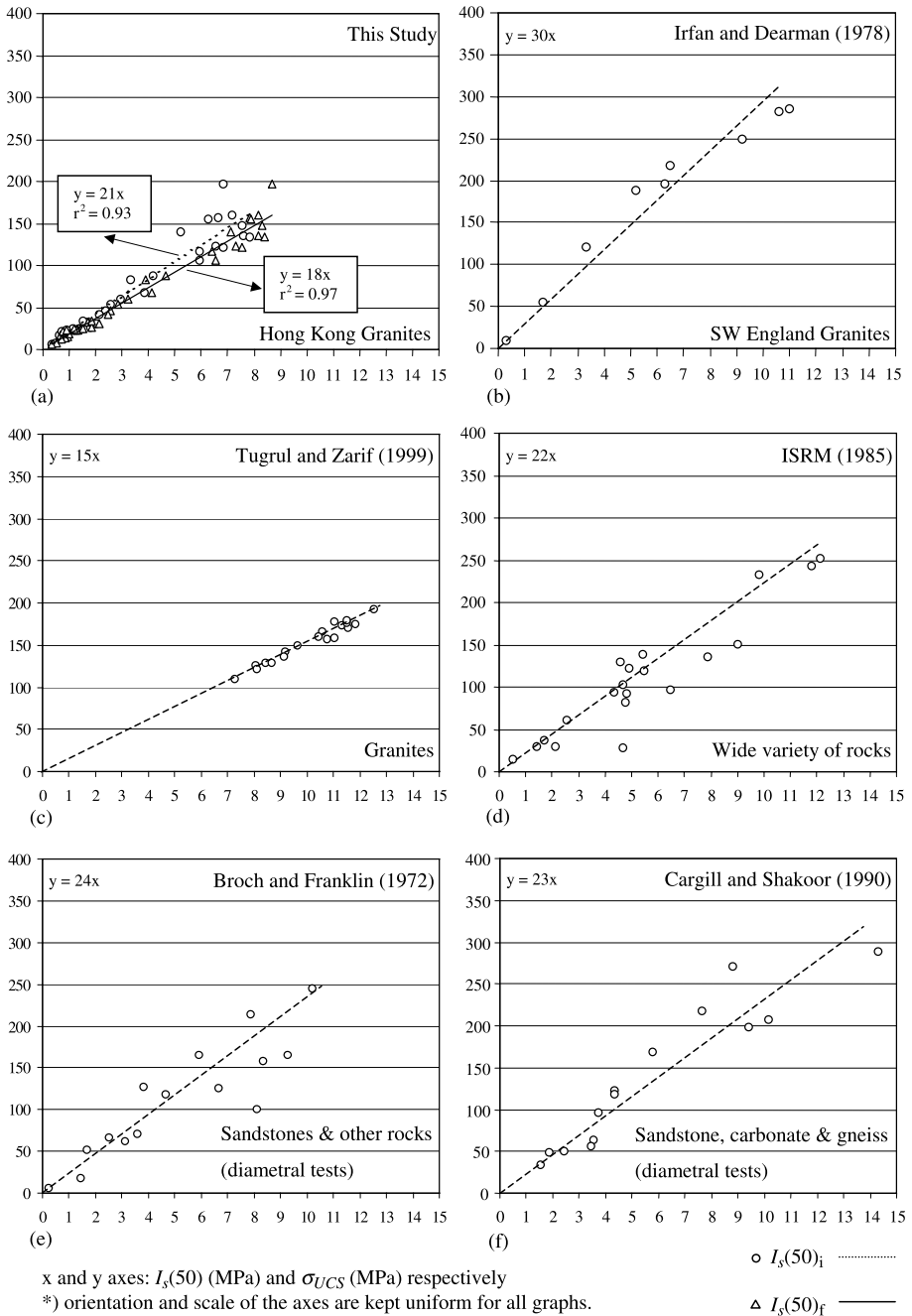


Fig. 2. Correlations between $I_s(50)$ and UCS: **a** This Study, **b** Irfan and Dearman (1978), **c** Tugrul and Zarif (1999), **d** ISRM (1985), **e** Broch and Franklin (1972), **f** Cargill and Shakoor (1990)

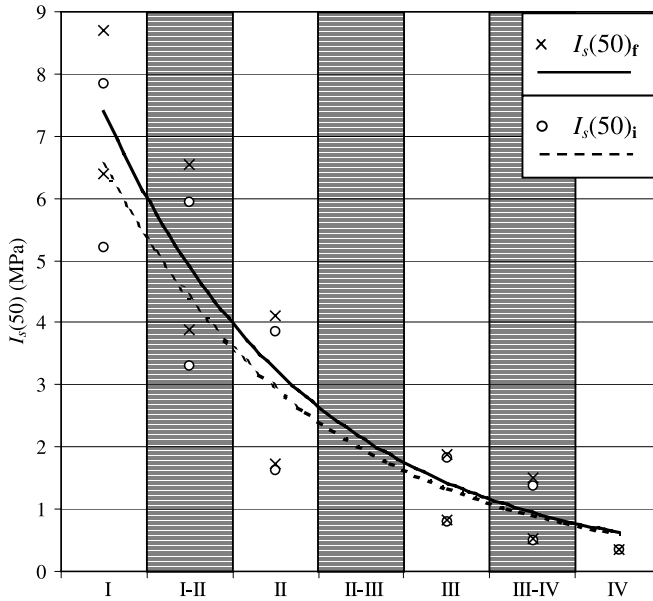


Fig. 3. Trends of initial and final $I_s(50)$ with weathering grades

significant improvements in these correlations could be achieved using the proposed test set up with automatic distance gage, as demonstrated in this study.

The ranges of $I_s(50)$ values within each weathering grade interval were determined and plotted against the corresponding grade (Table 2). It was noticed that both $I_s(50)_i$ and $I_s(50)_f$ values decay exponentially with the increasing degree of weathering, and that noticeable overlaps exist between the adjacent grades (Fig. 3, excluding specimen nos. 37–40). The degree of overlap was significantly lesser for $I_s(50)_f$, especially in Grade I to II specimens, which are still strong. Thus, the resolution and reliability of point load strength index to help differentiate early stages of weathering increases with accurate measurement of D at failure.

The average grain size of each specimen was determined with the help of the image analysis software *analySIS*® in order to investigate the influence of grain size on $I_s(50)$ (Table 2). It was noted that $I_s(50)$ values become extremely inconsistent with respect to weathering grades for specimen nos. 37–40. In spite of being compositionally similar to the others, these specimens displayed considerably higher $I_s(50)$ values than their coarser grained equivalents because of their finer grain sizes. Specimens with significant differences in grain size should therefore be evaluated separately, despite their compositional similarities, to optimize the efficacy of $I_s(50)$ as indicator or confirmatory tool for weathering grades.

4. Conclusions

The common standards (ISRM and ASTM) indicate that the cone penetration depth should be considered in determining $I_s(50)$ particularly for weak rocks. However, accu-

rate measurements of cone penetration depth by a laser distance sensor attached to a point load frame revealed that deeper penetration occurs in fresher/stronger rocks and when the penetration depth is considered, the scatter in the data is minimized leading to a significantly better regression coefficient and lower conversion factor for $I_s(50)_f$ in predicting UCS. The UCS vs. $I_s(50)_i$ correlation curves from the literature confirm that the scatter in the data lie mainly in the higher UCS range. The UCS value below which the depth of penetration has little or practically no influence on the correlations largely depends on the rock type and its microstructure. Therefore, the standards should acknowledge that the cone penetration could be significant particularly for fresher/stronger rocks.

In brittle rocks, penetration depth should decrease with decreasing tensile strength but the rate of change in depth may be smaller in fine grained rocks. Thus, specimens with significant differences in grain size should be evaluated separately, despite their compositional similarities, to enhance the efficacy of $I_s(50)$ as a predictive tool for UCS and as an indicator of weathering grades or for objective confirmation of their visual identification.

Acknowledgements

The work was financially supported by the Research and Conference Grants Committee of The University of Hong Kong. The authors gratefully acknowledge the technical assistance provided by Mr. Alan Kwok of the Department of Earth Sciences.

References

- ASTM (American Society for Testing and Materials) (2001): Standard method for determination of the point load strength index of rock, Designation D 5731–5795.
- Broch, E., Franklin, J. A. (1972): The point-load strength test. *Int. J. Rock Mech. Min. Sci. Geomech. Abstr.* 9, 669–697.
- Brook, N. (1985): The equivalent core diameter method of size and shape correction in point load testing. *Int. J. Rock Mech. Min. Sci. Geomech. Abstr.* 22, 61–70.
- Cargill, J. S., Shakoor, A. (1990): Evaluation of empirical methods for measuring the uniaxial compressive strength of rock. *Int. J. Rock Mech. Min. Sci. Geomech. Abstr.* 27, 495–503.
- Chau, K. T., Wong, R. H. C. (1996): Uniaxial compressive strength and point load strength. *Int. J. Rock Mech. Min. Sci. Geomech. Abstr.* 33, 183–188.
- Irfan, T. Y., Dearman, W. R. (1978): Engineering classification and index properties of a weathered granite. *Bull. Int. Assoc. Eng. Geol.* 17, 79–90.
- ISRM (International Society for Rock Mechanics). (1985): Suggested method for determining point load strength. *Int. J. Rock Mech. Min. Sci. Geomech. Abstr.* 22, 51–60.
- Reichmuth, D. R. (1968): Point-load testing of brittle materials to determine tensile strength and relative brittleness. In: *Proc., 9th Symposium on Rock Mech.* 134–159.
- Tugrul, A., Zarif, I. H. (1999): Correlation of mineralogical and textural characteristics with engineering properties of selected granitic rocks from Turkey. *Eng. Geol.* 51, 303–317.
- Wijk, G. (1978): Some new theoretical aspects of indirect measurements of the tensile strength of rocks. *Int. J. Rock Mech. Min. Sci. Geomech. Abstr.* 15, 149–160.

Authors' address: Dr. Adnan Aydin, Department of Earth Sciences, University of Hong Kong, Pokfulam Road, Hong Kong, SAR, China; e-mail: aaydin@hku.hk